Electronic Supplementary Information (ESI)

# Ultra-selective and Stable Ethylene Detection via Exsolution of Catalytic Ni Nanoparticles in Chemiresistive Gas Sensors

*Jieon Lee,[a,c] Yong Jung Kwon,[a] Hyeunseok Choi,[b] Soo Young Kim,[c] Jung-Hoon Lee,[d,e,*] and Young Kyu Jeong[a,*]*

[a]*Functional Materials & Components R&D group, Korea Institute of Industrial Technology (KITECH), 137-41 Gwahakdanji-ro, Gangneung-si, Gangwon 25440, Republic of Korea.*
[b]*Regional industrial innovation sector, Korea Institute of Industrial Technology (KITECH), 89, Yangdaegiro-gil, Ipjang-myeon, Seobuk-gu, Cheonan-si, Chungcheongnam-do, 31056, Republic of Korea.*
[c]*Department of Materials Science and Engineering, Korea University, 145, Anam-ro, Seongbuk-gu, Seoul, Republic of Korea, Seoul 02841, Republic of Korea.*
[d]*Computational Science Research Center, Korea Institute of Science and Technology (KIST), 5, Hwarang-ro 14-gil, Seongbuk-gu, Seoul, Republic of Korea, Seoul 02792, Republic of Korea.*
[e]*KU-KIST Graduate School of Converging Science and Technology, Korea University, Seoul 02841, Republic of Korea*

**Corresponding author, E-mail:* jhlee84@kist.re.kr, immrc80@gmail.com

## Experimental Section

### *Synthesis of ZnO nanoflowers*

Pure ZnO nanoflowers were synthesized using a co-precipitation method. To produce pure ZnO nanoflowers, zinc(Ⅱ) nitrate hexahydrate (0.8028 g, $Zn(NO_3)_2 \cdot 6H_2O$, 98.0%, Sigma-Aldrich) and Trisodium citrate dihydrate (2.118 g, $C_6H_5Na_3O_7 \cdot 2H_2O$, ≥99.0%, Sigma-Aldrich) were dissolved in deionized water (60 mL). The solution was then stirred for 10 minutes at room temperature. Subsequently, sodium hydroxide (0.6 g, NaOH, 98.0%, Sigma-Aldrich) was added to the solution and stirred for 1 hour at the same temperature. The precipitate was collected via centrifugation, washed several times with deionized water and absolute ethanol, and dried at 80 °C overnight. The powders were then calcined in air at 500 °C for 1 hour, resulting in the formation of pure ZnO nanoflowers (denoted as Ni0-ZnO).

### *Exsolution of Ni nanoparticles on ZnO nanoflowers*

For the synthesis of Ni-exsolved ZnO sample, the Ni-doped ZnO nanoflowers were initially prepared using the same method described above in the desired molar proportion between zinc(Ⅱ) nitrate hexahydrate and nickel(Ⅱ) nitrate hexahydrate($Ni(NO_3)_2 \cdot 6H_2O$, 99.9%, Sigma-Aldrich). After all the above processes in the same manner, the prepared powder was placed in an alumina boat, and additional heat treatment was performed at 600 °C for 1 hour in a reductive environment (5% $H_2$ / 95% Ar). Finally, ZnO nanoflower powder with Ni nanoparticles exsoluted on the surface was obtained. According to the Ni concentration in ZnO, they are named Ni1-ZnO, Ni3-ZnO, Ni5-ZnO, Ni7-ZnO, and Ni10-ZnO.

### *Fabrication of sensing films*

The sensing film was produced by drop coating on interdigitated electrodes (IDE) with an electrode gap of 5 μm. For drop coating, the synthesized Ni-exsolved ZnO

nanoflower powder was mixed with DMF (5% w/v) and sonicated for 5 minutes to prepare a coating solution. The number of droplets was adjusted to control the film thickness (30, 60, 100, 200, 300, and 400 μm). After coating, organic chemicals were removed by calcination in air at 500 °C with a heating rate of 3 °C/min for 1 hour.

***Computational details***

To elucidate the reaction pathway of ethylene on NiO and its adsorption properties on ZnO, we performed first-principles DFT calculations with the Vienna ab-initio simulation package (VASP) code.[1–4] To incorporate the influence of van der Waals (vdW) dispersive interactions on binding energies, structural relaxations were performed using the revised vdW-DF2 exchange-correlation functional implemented in VASP.[5] We employed a (i) 6×6×1 (3×3×1) k-point sampling of the Brillouin zone for the NiO and ZnO unit-cell (supercell) slabs and (ii) 500-eV plane-wave cutoff energy. According to our calculations, the surface energy of the NiO(001) plane was the most stable among the three planes (Table S3†).

Twelve, ten, six, four, and one valence electrons were explicitly treated for Zn ($3d^{10}4s^2$), Ni ($3d^8 4s^2$), O ($2s^2 2p^4$), C ($2s^2 2p^2$), and H($1s^1$), respectively. The ions were relaxed until the Hellmann–Feynman forces were below 0.01 eVÅ$^{-1}$. All NiO slabs were assumed to have antiferromagnetic ordering along the [111] direction, as reported experimentally.[6] We selected a Hubbard U value of 7.5 and 6.4 eV for Zn and Ni 3d states, respectively, following a previous study.[7,8] Using the above input parameters, both the unit cell volume and internal coordinates of the bulk structures were fully relaxed. For slab geometries, only three atomic layers from the surface were relaxed. The other atomic layers of NiO(001) and ZnO(100) slabs were set as 15-Å and 20-Å vacuum layers, respectively.

To compute the binding energies of ethylene, ethylene oxide, and acetaldehyde, we used dipole corrections to optimize the NiO(001) and ZnO(100) slabs ($E_{NiO,ZnO}$), ethylene, ethylene oxide, and acetaldehyde molecules in the gas phase ($E_{mol}$) within a 30 Å × 30 Å × 30 Å cubic supercell. The NiO (001) and ZnO (100) slabs with adsorbed

ethylene, ethylene oxide, and acetaldehyde molecules ($E_{mol-NiO,ZnO}$) were optimized using dipole corrections. The binding energies ($E_B$) were obtained from the difference as follows:

$$E_B = E_{mol-NiO,ZnO} - (E_{NiO,ZnO} + E_{mol}). \quad (1)$$

For binding energy calculations, we also only relaxed adsorbates and three atomic layers from a NiO(001) surface of the $2\sqrt{2} \times 2\sqrt{2} \times 1$ supercell slab and a ZnO(100) surface of the $3 \times 2 \times 1$ supercell slab while fixing the other atomic layers and cell parameters. Furthermore, we optimized the slab thickness of the NiO(001) and ZnO(100) slabs to achieve convergence of the surface energies with the convergence threshold of 0.02 eV per Å$^2$.

***Material Characterizations.***

The morphology of the Ni-exsolved ZnO nanoflowers was characterized using SEM (Quanta 250 FEG, FEI, USA), TEM (Philips CM-200, FEI, USA), and energy-dispersive X-ray spectroscopy (EDX). The phases and crystal structures of the samples were investigated using XRD (Empyrean, PANalytical, Netherlands) and analyzed using HighScore from Malvern PANalytical. The chemical states and compositions were analyzed using XPS (Thermo Scientific, K Alpha+, U.K.). To analyze the catalytic activity, the nanoflower powder (50 mg) was placed on a quartz wool and loaded into the center of a quartz tube reactor (length: 490 mm, inner diameter: 6.84 mm) located inside the furnace. The total flow rate of the reaction gas and gas hourly space velocity were fixed at 100 ml/min and 120,000 ml/g·h, respectively. The reactant and byproduct gases were analyzed using gas chromatography (GC; ChroZen GC, YOUNG IN Chromass, Korea). Generally, conversion rate is defined as Conversion (%) = ($C_{A0}$-$C_A$) / $C_{A0}$ x 100%, where $C_{A0}$ (inlet) and $C_A$ (outlet) represent the gas concentration before and after the reaction, respectively.

***Gas-sensing measurements.***

To verify the sensor characteristics of the manufactured sensor, experiments were

conducted in a temperature-controlled chamber, as shown in Fig.11†. The gas flow rate was controlled using a Mass Flow Controller, and the total gas flow rate was consistently maintained at a flow rate of 500 $cm^3 \cdot m^{-1}$ to ensure experimental consistency. The concentration and humidity of the analyte gas were controlled by varying the ratio of analyte gas to dry air and passing the gas through a water bath before injecting it into the detection chamber. Gas detection tests were performed by monitoring the change in electrical resistance of the sensor at various temperatures (230–430 °C) and RH (0–80%) levels. The sensor resistance was measured using a semiconductor characterization analyzer (4200-SCS, Keithley, Keithley Instruments, LLC & Tektronix, Inc., USA), and the sensor temperature was controlled by applying voltage to the heater located at the bottom of the sensor using a temperature controller (MST1000H, MS TECH, Korea).

***Synthesis of control sample with chemical reduction method.***

In a typical process, 0.5 g of ZnO nanoflowers prepared by the above method were dispersed into 50 mL of deionized water by sonication for 30 minutes. Subsequently, the pH of the solution was adjusted to 10 with NaOH solution and stirred for 20 minutes. Afterwards, appropriate amounts of nickel(Ⅱ) nitrate hexahydrate ($Ni(NO_3)_2 \cdot 6H_2O$, 99.9%, Sigma-Aldrich) were added with continuous stirring for 4 hours. Finally, freshly prepared $NaBH_4$ aqueous solution (2 mg/mL) was added to the above mixture and stirred for another 45 minutes to complete the reduction of the metal precursor. The precipitate was collected via centrifugation, washed several times with deionized water and absolute ethanol, and dried at 80 °C overnight. The powders were then calcined in air at 500 °C for 1 hour in a furnace.

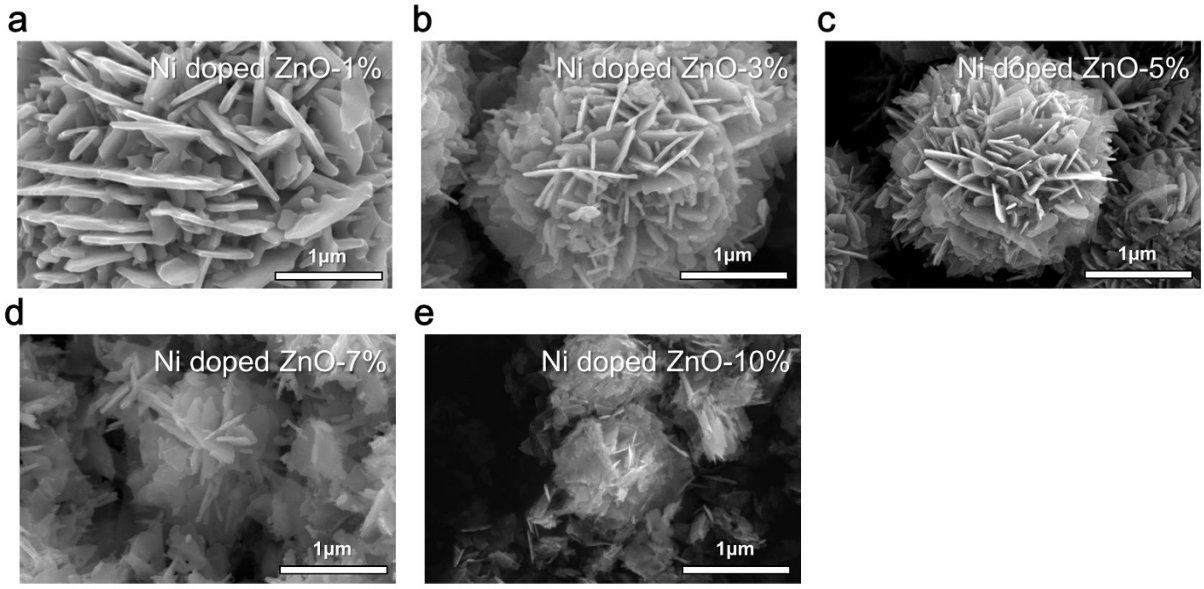


**Fig. S1** SEM images of (a)–(e) Ni-doped ZnO nanoflowers with various Ni concentrations prior to the exsolution process; (a) 1 at%, (b) 3 at%, (c) 5 at%, (d) 7 at% and (e) 10 at% of Ni.

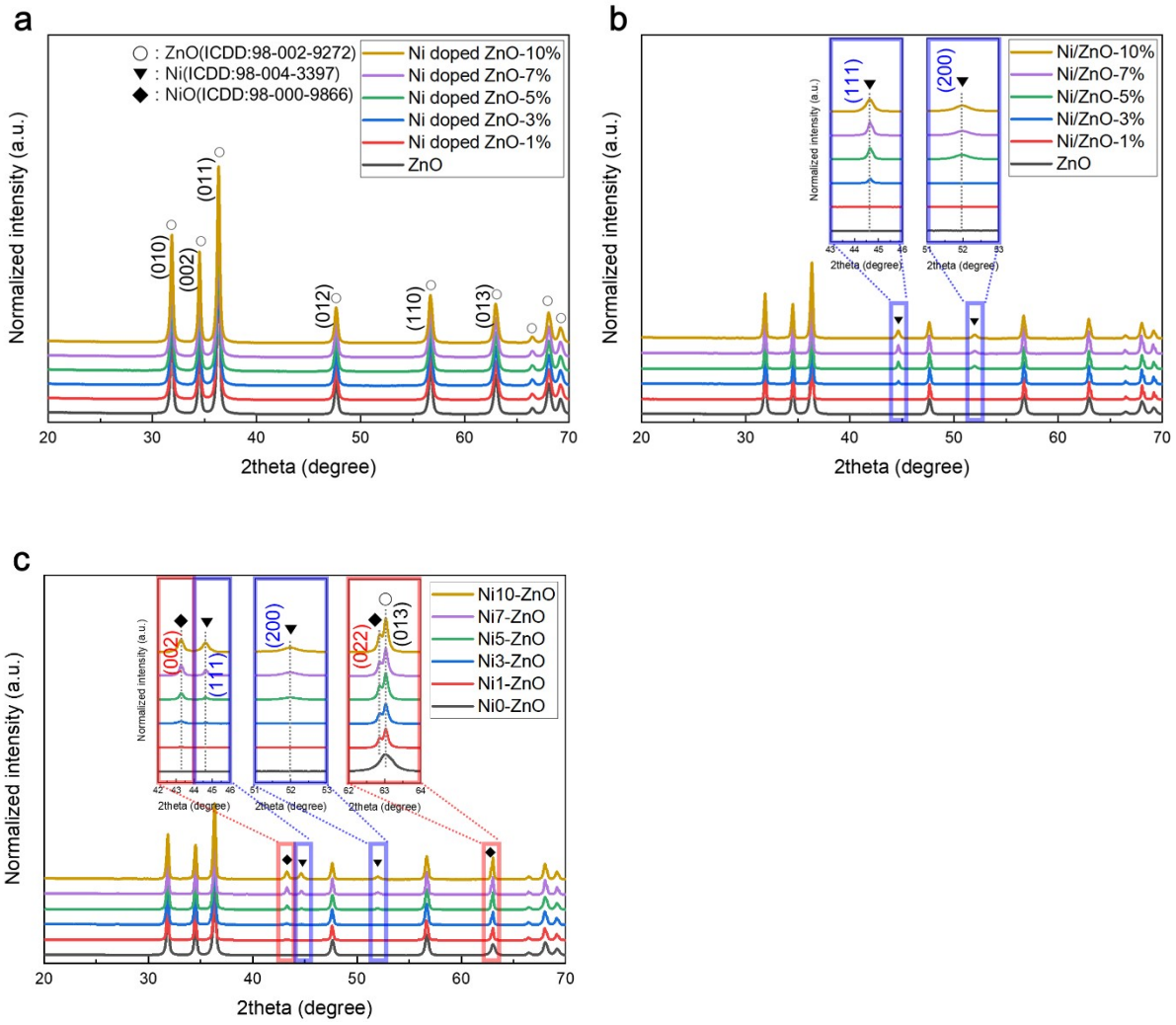


**Fig. S2** XRD patterns of Ni-doped ZnO nanoflowers (a) after calcination at 500 °C for 1hour, (b) reductive treatment for the exsolution of Ni nanoparticles at 600 °C for 1hour, and (c) gas sensing measurements at 380 °C.

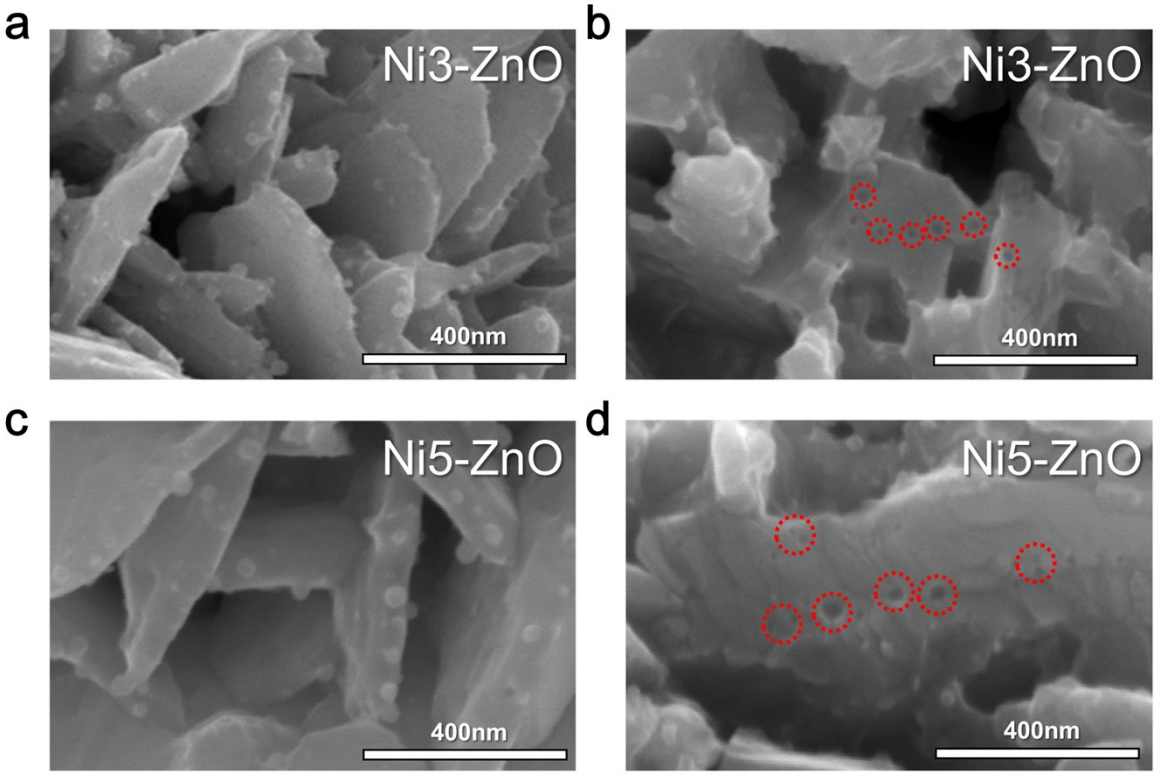


**Fig. S3** SEM images showing the surface topography of Ni3-ZnO and Ni5-ZnO after selective etching of exsoluted Ni nanoparticles with nitric acid.

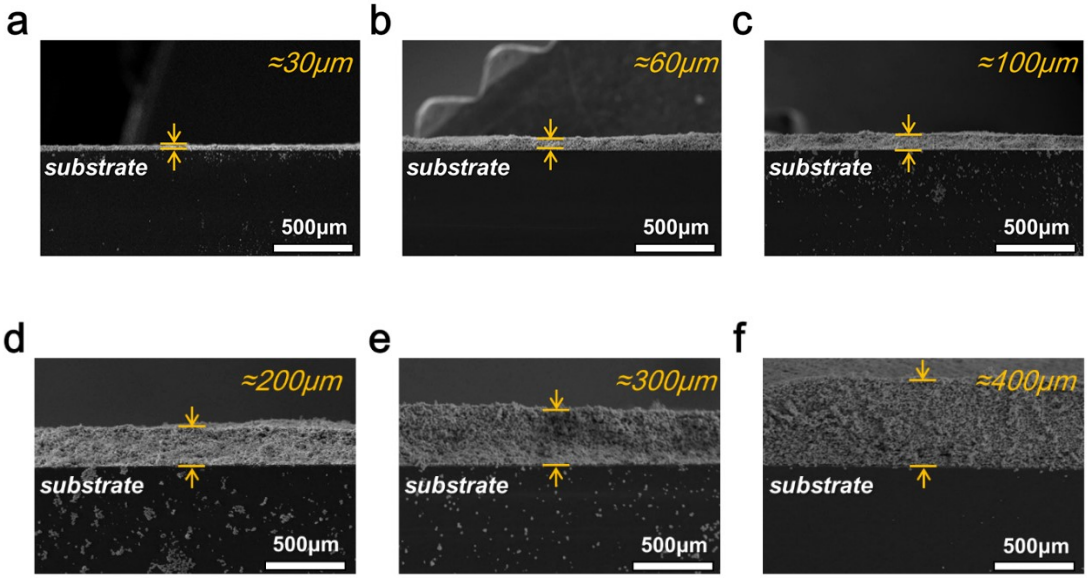


**Fig. S4** Cross-sectional SEM images of sensing films with various thicknesses from 30 to 400 μm.

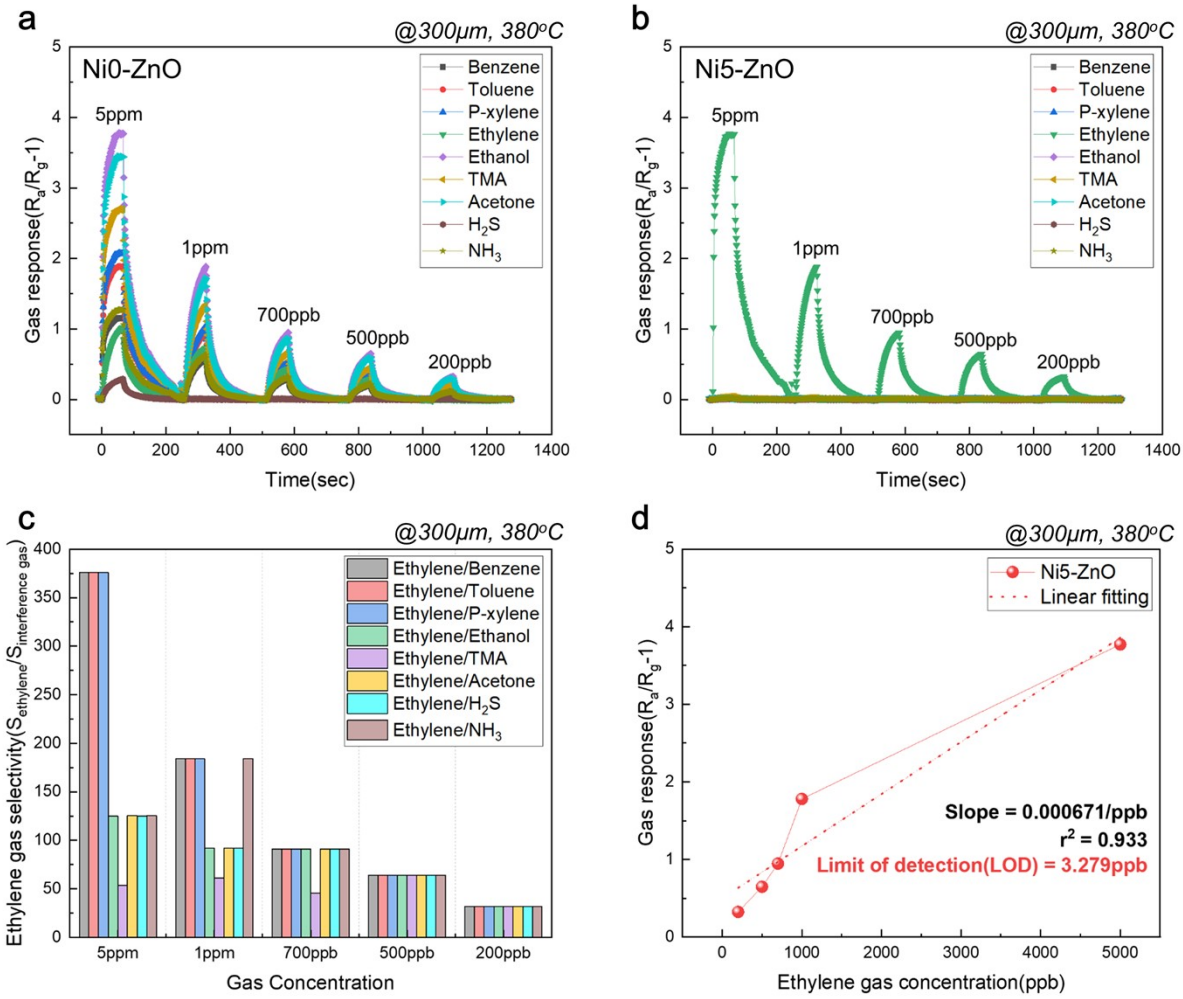


**Fig. S5** (a)-(b) Dynamic response curves of (a) Ni0-ZnO and (b) Ni5-ZnO sensors toward various gases (benzene, toluene, p-xylene, ethylene, ethanol, TMA, acetone, $H_2S$, $NH_3$) at different low concentrations at 380 °C. (c) ethylene selectivity over various interferents measured at 380 °C and (d) a calculated LOD value in the Ni5-ZnO sensor.

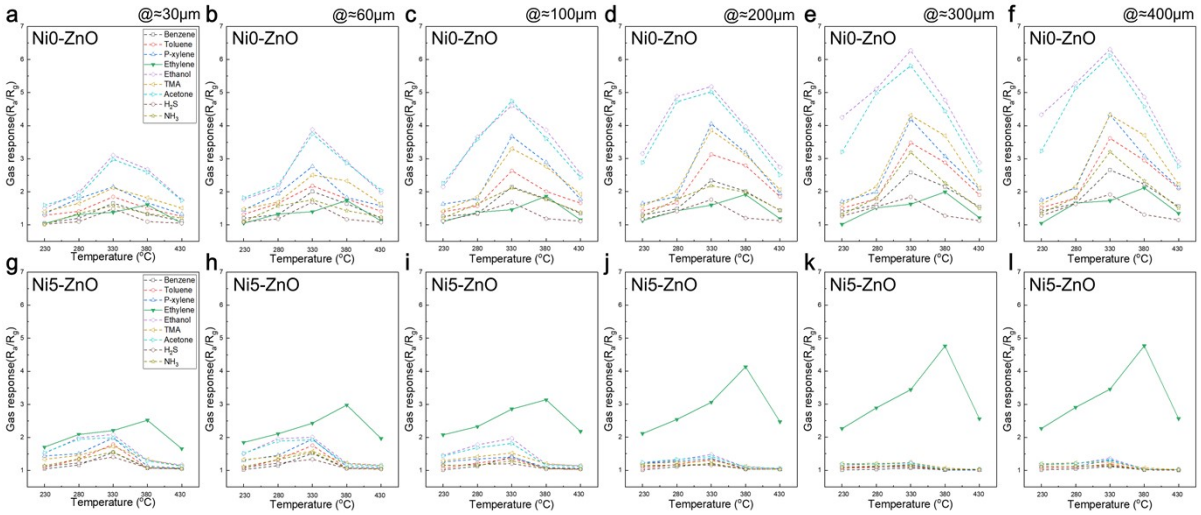


**Fig. S6** Variations of film thickness and its effects on the gas response as a function of temperature. Gas sensing characteristics of (a)-(f) Ni0-ZnO, (g)-(l) Ni5-ZnO sensors to nine gases (5 ppm-benzene, -toluene, -p-xylene, -ethylene, -ethanol, -TMA, -acetone, -$H_2S$, -$NH_3$) as a function of measurement temperature from 230 to 430 °C and coating film thickness from 30 to 400 μm.

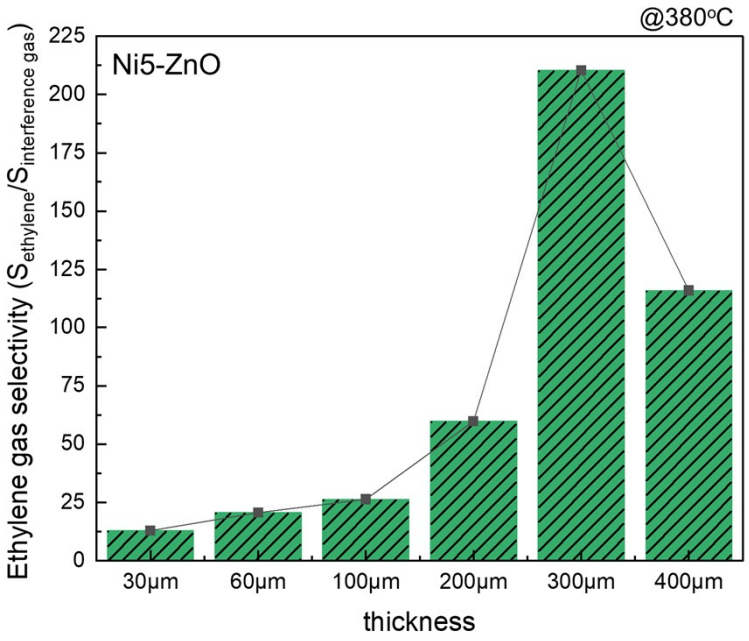


**Fig. S7** Average Selectivity of ethylene over the 9 interferents at 380 °C as a function of the coating film thickness (Ni5-ZnO sensor).

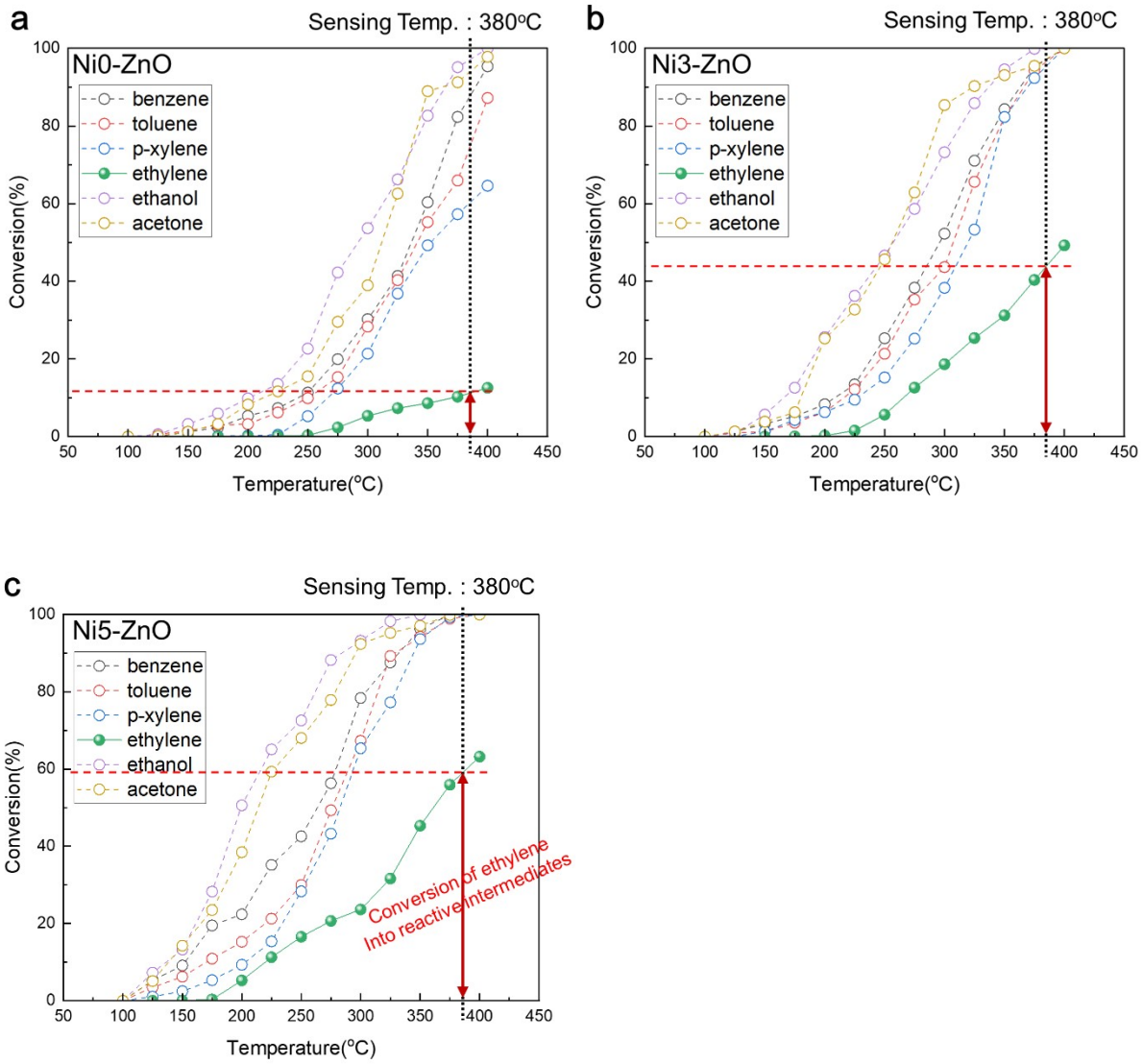


**Fig. S8** (a)-(c) Catalytic conversion of several analyte gases (5ppm) over (a) Ni0-ZnO, (b) Ni3-ZnO, (c) Ni5-ZnO in the temperature range of 100 to 400 °C.

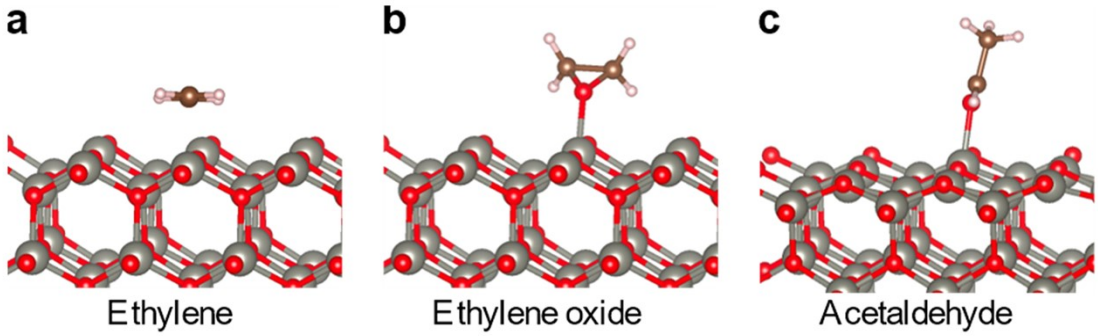


**Fig. S9** DFT-optimized structures of (a) ethylene-, (b) ethylene oxide-, and (c) acetaldehyde-adsorbed on defect-free ZnO(100) surfaces.

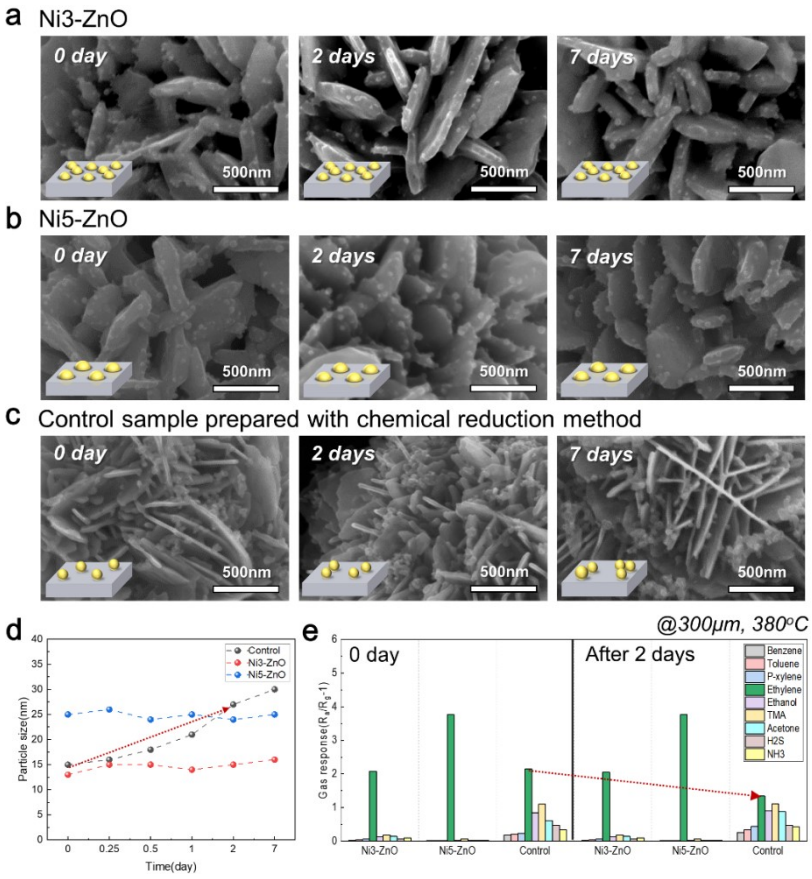


**Fig. S10** SEM images of (a) Ni3-ZnO, (b) Ni5-ZnO, and (c) control sample after long-term sensing evaluation for 0 to 7 days at 380 °C. (d) Changes in particle size of Ni in the sensors composed of Ni3-ZnO, Ni5-ZnO, and control sample, and (e) their relevant ethylene response (5 ppm) over evaluation time at 380 °C.

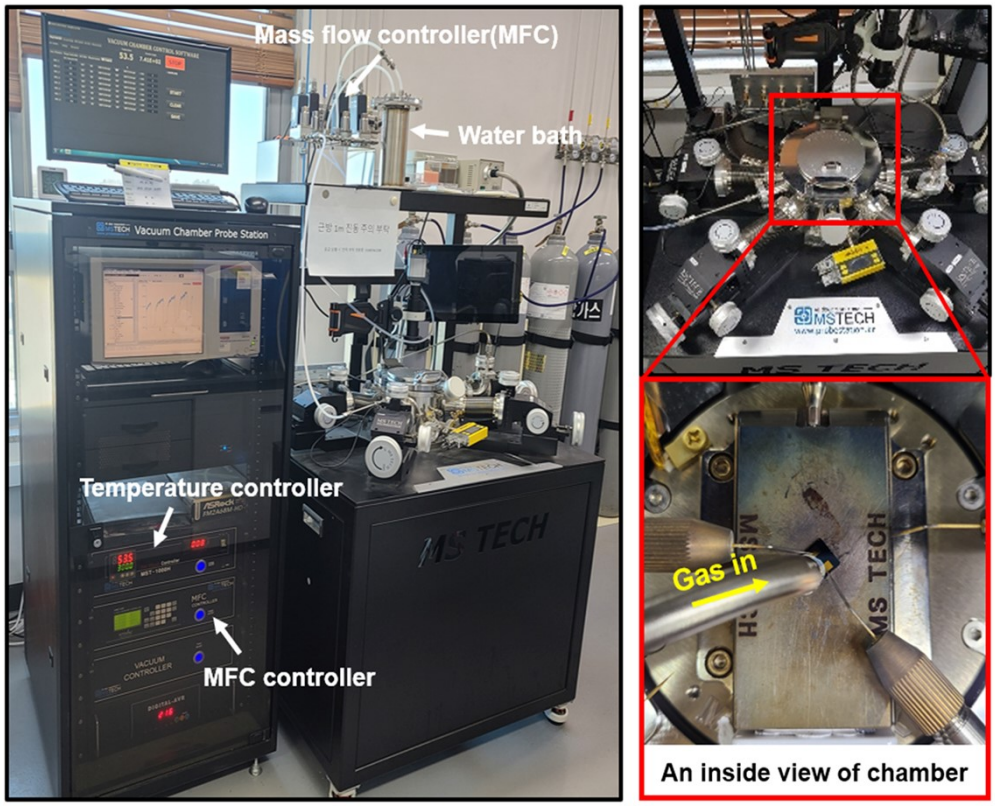


**Fig. S11** Gas sensing measurement system.

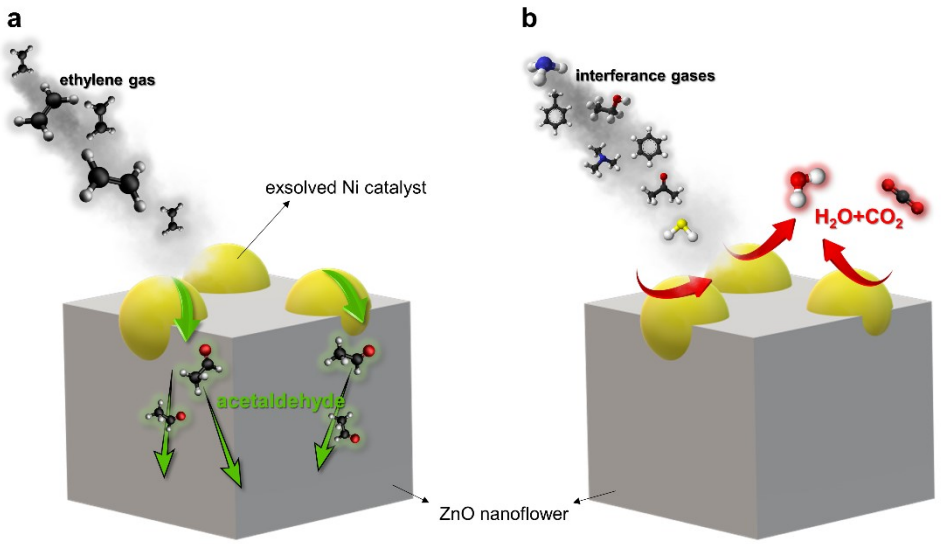


**Fig. S12** A schematic illustration regarding the ethylene detection mechanism in the Ni-ZnO sensor: catalytic reactions of (a) ethylene and (b) interference gases on the surface of Ni-ZnO sensors.

| | Ethylene | Ethylene oxide | Acetaldehyde |
|---|---|---|---|
| NiO(001) | -0.508 | 2.919 | 0.655 |
| NiO(001)-H | -0.443 | 2.960 | 0.847 |
| NiO(001)-OH | -0.304 | -0.262 | -1.713 |

**Table S1.** Computed binding energies $E_B$ (in eV) of ethylene, ethylene oxide, and acetaldehyde on NiO(001), NiO(001)-H, and NiO(001)-OH surfaces.

| | Ethylene | Ethylene oxide | Acetaldehyde |
|---|---|---|---|
| No defect | -0.587 | -0.906 | -0.801 |
| $V_O$ | -0.401 | -0.665 | -0.583 |
| $V_{Zn}$ | -0.236 | -0.895 | -0.957 |
| $V_{Zn-O}$ | -0.605 | -1.473 | -1.652 |

**Table S2.** Computed binding energies $E_B$ (in eV) of ethylene, ethylene oxide, and acetaldehyde on ZnO(100) surface with $V_O$, $V_{Zn}$, and $V_{Zn-O}$.

| | (001) | (110) | (111) |
|---|---|---|---|
| $E_S$ | 0.083 | 0.156 | 0.117 |

**Table S3.** Computed surface energies $E_S$ (in eV per Å$^2$) of NiO for the (001), (110), and (111) planes.

## References


1 G. Kresse and J. Hafner, *Phys. Rev. B*, 1993, **47**, 558–561.

2 G. Kresse and J. Furthmüller, *Phys. Rev. B*, 1996, **54**, 11169–11186.

3 G. Kresse and J. Furthmüller, *Comput. Mater. Sci.*, 1996, **6**, 15–50.

4 G. Kresse and J. Hafner, *Phys. Rev. B*, 1994, **49**, 14251–14269.

5 I. Hamada, *Phys. Rev. B*, 2014, **89**, 121103.

6 A. Barbier, C. Mocuta, W. Neubeck, M. Mulazzi, F. Yakhou, K. Chesnel, A. Sollier, C. Vettier and F. de Bergevin, *Phys. Rev. Lett.*, 2004, **93**, 257208.

7 P. Erhart, K. Albe and A. Klein, *Phys. Rev. B - Condens. Matter Mater. Phys.*, 2006, **73**, 1–9.

8 L. Wang, T. Maxisch and G. Ceder, *Phys. Rev. B*, 2006, **73**, 195107.